

Airborne transmission of COVID-19 and mitigation using box fan air cleaners in a poorly ventilated classroom

Cite as: Phys. Fluids **33**, 057107 (2021); doi: [10.1063/5.0050058](https://doi.org/10.1063/5.0050058)

Submitted: 11 March 2021 · Accepted: 2 April 2021 ·

Published Online: 11 May 2021






View Online



Export Citation



CrossMark

Ruichen He (何瑞辰),^{1,2}  Wanjiao Liu (刘婉娇),³ John Elson,³ Rainer Vogt,⁴ Clay Maranville,³ 
and Jiarong Hong (洪家荣)^{1,2,a)} 

AFFILIATIONS

¹Department of Mechanical Engineering, University of Minnesota, Minneapolis, Minnesota 55455, USA

²Saint Anthony Falls Laboratory, University of Minnesota, Minneapolis, Minnesota 55414, USA

³Research and Advanced Engineering, Ford Motor Company, 2101 Village Road, Dearborn, Michigan 48121, USA

⁴Ford-Werke GmbH, Research & Innovation Center, 52072 Aachen, Germany

Note: This paper is part of the special topic, Flow and the Virus.

^{a)}Author to whom correspondence should be addressed: jhong@umn.edu

ABSTRACT

Many indoor places, including aged classrooms and offices, prisons, homeless shelters, etc., are poorly ventilated but resource-limited to afford expensive ventilation upgrades or commercial air purification systems, raising concerns on the safety of opening activities in these places in the era of the COVID-19 pandemic. To address this challenge, using computational fluid dynamics, we conducted a systematic investigation of airborne transmission in a classroom equipped with a single horizontal unit ventilator (HUV) and evaluate the performance of a low-cost box fan air cleaner for risk mitigation. Our study shows that placing box fan air cleaners in the classroom results in a substantial reduction of airborne transmission risk across the entire space. The air cleaner can achieve optimal performance when placed near the asymptomatic patient. However, without knowing the location of the patient, the performance of the cleaner is optimal near the HUV with the air flowing downwards. In addition, we find that it is more efficient in reducing aerosol concentration and spread in the classroom by adding air cleaners in comparison with raising the flow rate of HUV alone. The number and placement of air cleaners need to be adjusted to maintain their efficacy for larger classrooms and to account for the thermal gradient associated with a human thermal plume and hot ventilation air during cold seasons. Overall, our study shows that box fan air cleaners can serve as an effective low-cost alternative for mitigating airborne transmission risks in poorly ventilated spaces.

Published under license by AIP Publishing. <https://doi.org/10.1063/5.0050058>

I. INTRODUCTION

Increasing evidence has shown that airborne transmission is an important pathway that leads to the spread of COVID-19.¹⁻⁴ Compared to outdoor settings, the risk of airborne transmission is significantly higher for various congregated indoor activities.⁵⁻⁷ Improved ventilation has been commonly recommended as an important preventive measure to reduce the risk of indoor airborne transmission.⁸ By replacing contaminated air with clean air, ventilation can help lower the concentration of particulate matters and reduce the probability of exposure to virus-containing aerosols.^{9,10} Particularly, one study has shown that a low infection probability of less than 1% can be achieved with a ventilation rate above typical recommended values.¹¹ However, many indoor spaces are poorly ventilated, including a large number of old public-school classrooms^{11,12} and offices.¹³

These classrooms are especially prone to higher risks of airborne transmission, due to aged infrastructure, high population density, and extended hours of operation that can lead to high levels of aerosol accumulation. Studies have shown that opening a window is an effective approach to alleviate aerosol accumulation¹⁴ but is hard to implement during cold/hot seasons, and many classrooms have no operable windows. Another suggested mitigation approach is to upgrade the existing central heating, ventilation, and air conditioning (HVAC) system,¹⁵ but the high cost impedes its implementation in resource-limited indoor spaces.

As an alternative approach, portable air purifiers are broadly used for risk mitigation in these poorly ventilated spaces.¹⁶ It has been recently demonstrated in a classroom with no ventilation that the usage of high-efficiency particulate air (HEPA) grade purifiers can

significantly reduce the aerosol concentration level.¹⁷ Nevertheless, the commercial purifiers used for public spaces such as classrooms and shared offices typically require a clean air delivery rate (CADR) of larger than 400 cfm¹⁸ with price ranging from \$400 to above \$4000.¹⁹ Such high costs limit the wide adoption of this mitigation approach, particularly in resource-limited indoor places,^{10,14} including public schools, prisons, downmarket offices, shelters, life care centers, etc. To cope with this challenge, a low-cost air cleaner constructed using readily available air filter panels and a box fan was proposed.²⁰ Unlike its commercial counterparts, the performance of this low-cost system had not previously been evaluated in a systematic fashion.

Therefore, using the computational fluid dynamics (CFD) approach, our current study aims to provide a systematic assessment of using these low-cost air cleaners as an alternative approach for risk mitigation in poorly ventilated indoor spaces. Since the outbreak of severe acute respiratory syndrome (SARS) in 2003, CFD has been employed as an effective tool to assess airborne transmission risks under various indoor and outdoor settings.^{21–25} Particularly, Lin *et al.*²⁶ first simulated airborne transmission due to coughing in a well-ventilated classroom with 12 air exchange per hour (ACH) under different ventilation designs and showed that mixing ventilation leads to the highest aerosol concentration compared to displacement and stratum ventilation designs. Using a classroom of similar size (under 7.5 ACH), Zhang *et al.*²⁷ investigated transmission caused by continuous talking and demonstrated the superiority of displacement over mixing ventilation in lowering aerosol concentration and spread. Abuhegazy *et al.*²⁸ systematically evaluated the effect of the location of an asymptomatic individual (referred to as infector hereafter) and the size of particles generated by the infector on airborne transmission in a well-ventilated classroom (8.6 ACH) with distributed ventilation. They showed a substantial fraction (24%–50%) of particles can be removed by the ventilation and opening the window can further increase the fraction of removal to 69%. In contrast, in a classroom with a single site ventilation, Shao *et al.*²⁹ showed that ventilation can only extract a small fraction of aerosols (~3%) even under an exceedingly high ventilation (i.e., 30 ACH) with a majority of aerosols depositing on surfaces due to the presence of stable flow circulation regions in the space.

Despite these past efforts, very few studies focused on airborne transmission in poorly ventilated classrooms. These classrooms are widely present in public schools.³⁰ They are usually equipped with a single horizontal unit ventilator (HUV, unit ventilator is the most common type of HVAC system used in public schools) operating at air exchange rate of around 2 ACH, significantly lower than the ventilation used in above-mentioned investigations. Furthermore, as pointed out earlier, no study has systematically evaluated these low-cost air cleaners including the influence of placement and design on their performance, although some have studied the location effect of the air cleaner under other settings.^{31,32}

To fill in this gap, our study focuses on investigating the airborne transmission under poorly ventilated classroom settings and the efficacy of the corresponding mitigation strategies using low-cost box fan air cleaners. The work is conducted using CFD with air cleaner models characterized using experiments. The present paper is structured as follows: Sec. II describes the design of our simulation including the design and characterization of low-cost air cleaner model and the setups of different simulation cases. Successively, in Sec. III, we present our simulation results evaluating the influence of the placement and

flow direction of air cleaners, room size as well as the thermal gradient in the air on the air cleaner performance. The results are also compared with those from the simulation cases using only enhanced ventilation (no air cleaner placed in the room). Finally, the conclusions and discussions are provided in Sec. IV.

II. METHODOLOGY

A. Box fan air cleaner model

The low-cost box fan air cleaner used in the study is designed and constructed by Ford.³³ As shown in Figs. 1(a) and 1(b), the air cleaner is comprised of an easy-to-assemble die-cut cardboard support, a box fan of 0.5×0.5 m² cross section, and a $0.5 \times 0.5 \times 0.1$ m³ air filter with a standard minimum efficiency reporting value (MERV) of 13. The filter panel is placed inside the folded base with the fan placed on top. The fan operates on high for maximum filtration, discharging clean air downward as it pulls in unfiltered air from above.

To characterize the flow rate and inlet velocity profile of the box fan air cleaner, a vane anemometer (OMEGA) is used to measure the velocity at 35 locations distributed at the inlet surface of the box fan air cleaner [Fig. 2(a)]. The inlet velocity profile is found to be nearly uniform over 80% of the total area in the center as shown in Fig. 2(b), with an average velocity of 1.5 m/s with a standard deviation of 0.2 m/s. Based on these measurements and the area of the measurement location (35×7 cm diameter holes), the total flow rate is calculated to be about 0.2 m³/s. Accordingly, for simplification, we use a flow rate of 0.2 m³/s and a uniform inlet velocity profile for the air cleaner model in the simulations. To visualize the efficacy of the box fan air cleaner in extracting the small particles (~ 1 μ m), a supplementary video (supplementary material Video 1) is captured using an electron-multiplying CCD camera which can capture the weak signal of micrometer size particles in a large area around 1 m scale. To evaluate the filtration performance of the filter panel used in the box-fan air cleaner, the commercially available air filter panel (Tri-Pleat Green 20204SP, Tri-Dim Mann & Hummel) performance is measured using the ASHRAE 52.2–2017 test standard³⁴ at an independent test lab using KCl as the challenge aerosol, which reported performance exceeding the MERV 13 performance standard. Therefore, in the simulation, we set the filtration efficiency of the air cleaner to be 100% for simplification. To assess the CADR of the air cleaner, two experiments are conducted at two independent laboratories following the ANSI/AHAM AC-1 test standard³⁵ using tobacco smoke as the challenge particle. Tobacco smoke CADR is reported as 213 cfm (362 m³/h) in the first lab and 231 cfm (392 m³/h) at the second lab. The difference in performance is likely due to setup and measurement differences.

B. Numerical simulation

CFD simulation is conducted using OpenFOAM-2012 platform, with the Eulerian–Lagrangian framework for simulating gas-particle phases. In the simulation, unsteady Reynolds-averaged Navier–Stokes (URANS) is performed. The implicit unsteady shear stress transport k - ω turbulence model is used with low Reynolds number modification to model the flow turbulence, which has been used in previous studies investigating the aerosol dispersion from human respiratory activities.^{36–38} Air flow is calculated using a compressible solver to model the buoyancy forces based on the following equations:

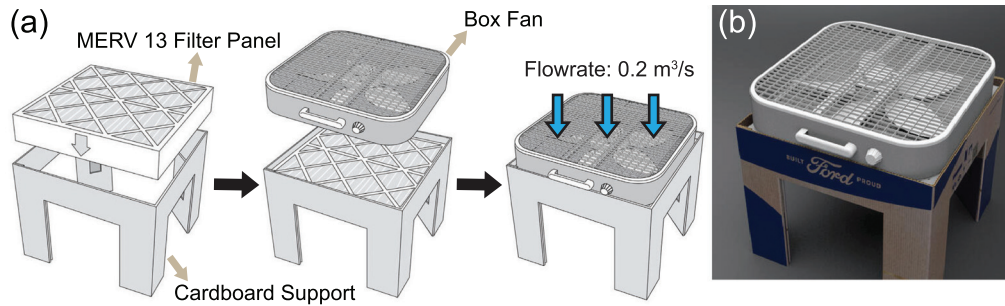


FIG. 1. (a) Schematic showing the composition and assembly procedure of the box fan air cleaner designed by Ford. (b) Photo of the box fan air cleaner.

$$\frac{\partial \rho_f}{\partial t} + \nabla \cdot (\rho_f \mathbf{U}) = 0,$$

$$\frac{\partial \mathbf{U}}{\partial t} + \nabla \cdot (\mathbf{U}\mathbf{U}) = -\nabla p_{\text{rgh}} - (\mathbf{g} \cdot \mathbf{x}) \nabla \left(\frac{\rho_f}{\rho_0} \right) + \nabla \cdot (2\nu_{\text{eff}} D(\mathbf{U})),$$

$$\frac{\partial \rho_f h}{\partial t} + \nabla \cdot (\rho_f \mathbf{U}h) = \nabla \alpha_{\text{eff}} \nabla h \rho_f + \frac{\partial p}{\partial t}.$$

In the equations, ρ_f is fluid density, \mathbf{U} represents the flow velocity, $\mathbf{g} = 9.81 \text{ m/s}^2$ is the gravity acceleration, \mathbf{x} is the position vector, ν_{eff} is the kinematic viscosity, h is the enthalpy, and ρ_0 is the reference density of the fluid at reference temperature T_0 . α_{eff} represents the effective thermal diffusivity. $D(\mathbf{U}) = \frac{1}{2} (\nabla \mathbf{U} + (\nabla \mathbf{U})^T)$ is the rate of strain tensor. p is the pressure field. The pressure under the assumption of the Boussinesq approximation, p_{rgh} , is defined as

$$p_{\text{rgh}} = (p - \rho_f \mathbf{g} \cdot \mathbf{x}) / \rho_0.$$

In the above equation, the fluid density ρ_f is calculated based on the following equation:

$$\rho_f = \rho_0 [1 - \beta \cdot (T_f - T_0)].$$

In the equation, the β is the volumetric thermal expansion coefficient and the T_f is the fluid temperature.

To handle the convective terms, the second-order upwind scheme is implemented. For the diffusion terms, the Gauss-linear second-order approach is used. For the coupling of the pressure and the

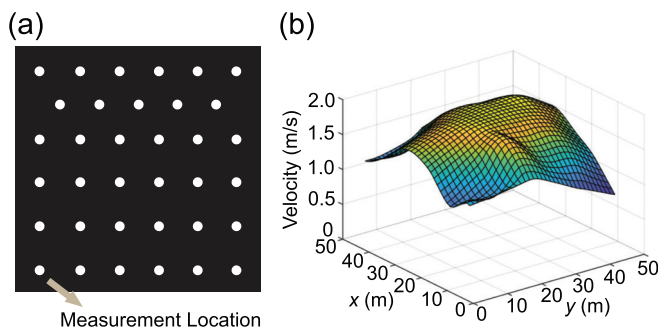


FIG. 2. (a) Schematic showing the locations of anemometer measurements used to characterize the inflow conditions of the box fan air cleaner. (b) Inlet velocity profile of the air cleaner obtained from the anemometer measurements.

velocity, the pressure-implicit with splitting of operator (PISO) algorithm is applied. The minimum residuals for the convergence of pressure, and velocity are 10^{-8} and 10^{-12} , respectively. The second-order Crank–Nicolson finite difference method is used for the time domain. The adjustable time step is employed with the maximum courant number of 0.7.

As for the particle movement simulation, one-way coupled Eulerian–Lagrangian approach is applied to predict the deposition and dispersion of each particle. Particles are assumed to be spherical and particle–particle interactions are ignored. The particle motion is tracked by using the time integration of Newton’s second law. The translational motion of each particle is governed by the Maxey–Riley equation. To determine the particle velocity $u_{i,p}$, and position $x_{i,p}$, such equation is solved for each particle, which is given by

$$\frac{d\mathbf{x}_{i,p}}{dt} = \mathbf{u}_{i,p},$$

$$m_{i,p} \frac{d\mathbf{u}_{i,p}}{dt} = F_i^D + F_i^L + F_i^{BM} + F_i^G.$$

In the equations, i is the particle ID, u_p is the particle velocity, m_p is the particle mass, F^D represents the drag force, F^L is the lift force, F^G is the gravitational force, and F^{BM} is the force induced by Brownian motion. The drag force uses the following form:

$$F^D = \frac{1}{8} C_D \pi d_p^2 |\vec{u}_f - \vec{u}_p| (\vec{u}_f - \vec{u}_p).$$

In the equation, d_p is the particle diameter and u_f is the velocity of the fluid. The drag coefficient, C_D , is determined by the following equation:

$$C_D = \begin{cases} 0.424 Re, & Re > 1000, \\ \frac{24.0}{Re} \left(1 + \frac{1}{6} Re^{\frac{3}{2}} \right), & Re \leq 1000. \end{cases}$$

The lift force is of the form,

$$F^L = \frac{2K\nu^{\frac{1}{2}} d_{ij}}{\rho_p d_p (d_{ik} d_{kl})^{\frac{1}{2}}} (\vec{u}_p - \vec{u}_f).$$

In the equation, $K = 2.594$ is the constant coefficient of Saffman’s lift force, ν is the kinematic viscosity, and ρ_p is the particle density. The density of water is used for ρ_p , as the particles are mostly water.³⁹ The deformation rate tensor, d_{ij} , is defined as

$$d_{ij} = \frac{1}{2} (u_{i,j} + u_{j,i}).$$

The Brownian motion induced force is of the following forms:

$$F^{BM} = m_p G_i \sqrt{\frac{\pi S_0}{\Delta t}},$$

with G_i are the zero-mean, unit variance independent Gaussian random numbers, Δt is the time step used in the simulation, and

$$S_0 = \frac{216\nu kT}{\pi^2 \rho_f d_p^5 \left(\frac{\rho_p}{\rho_f}\right)^2}.$$

In the equation, $k = 1.38 \times 10^{-23}$ J/K is the Boltzmann constant and T is the absolute temperature of the fluid. In the end, the gravity force, including the effect of buoyancy, is

$$F^G = m_p g \left(1 - \frac{\rho_f}{\rho_p}\right).$$

In the simulation, the turbulence effect is considered by modeling the dispersion of the particle using a stochastic model. The discrete random walk (DRW) model is used for the Lagrangian stochastic computation. The particles are made to interact with the instantaneous velocity field. The result velocity field will be used for the dispersion simulation of the particle. By this way, the flow's turbulence effect is considered in the simulation. To implement the function, the *StochasticDispersionRAS* model provided in the OpenFOAM library of the Lagrangian particle dispersion is utilized.

There are various forms of particle interactions. Only particle-wall interactions such as deposit and rebound are considered in the simulation. The standard wall interaction functions provided by OpenFOAM are implemented in the study to simulate the interaction between the particle and the wall patch, which has been validated in previous study in comparison with experiment data,⁴⁰ and have been used for different types of simulation studies.⁴¹

Table I summarizes all the simulation cases presented in the current study including (i) baseline cases (cases A and B), (ii) cases to evaluate the placement effect of air cleaner on their performance (cases A1–A4, cases B1–B4, and cases A12 and B12), (iii) cases to evaluate the inflow direction of air cleaners on their performance (cases FA2 and FB2), (iv) cases with only enhanced ventilation for comparison with the cases using air cleaners (cases VA and VB), (v) cases to evaluate the effect of room size on air cleaners' performance (cases LB, LB2, LB12, and LB22), and (vi) cases that include the thermal effect (cases TA2, TB2, TA2H, and TB2H). Specifically, for baseline cases, the computational domain is selected to simulate a classroom of $10 \times 5 \times 3$ m³, as shown in Fig. 3(a). The classroom is equipped with a horizontal unit ventilator (HUV) simplified as a $1.5 \times 0.8 \times 0.3$ m³ cuboid placed next to the wall [Fig. 3(b)]. The inlet [green area in Fig. 3(b)] and outlet [red area in Fig. 3(b)] dimensions of HUV are 1.2×0.05 m² and 1.2×0.1 m², respectively. An outlet pressure boundary condition is applied at the HUV inlet patch while a constant mass flow rate boundary condition is used for the outlet. The flow rate of the HUV is set as 325 cfm (0.15 m³/s, corresponding to 2 ACH for the simulated classroom size) with 50% filtration efficiency, which is used to simplify adding same amount of outside clean air with the recycled polluted

air. The room air temperature is set as 24 °C. Zero gradient temperature and no-slip wall boundary conditions are applied to all the wall in the domain. An asymptomatic instructor, referred to as the infector hereafter, is placed in the front (location A) or the middle (location B) of the classroom. The simulations are conducted over a 50-min duration with continuous particle injection at 110 particles per second⁴² with a mean diameter of 2 μm representing an asymptomatic instructor giving a 50-min lecture. The particle sizes are initialized with the Rosin-Rammler distribution, with the minimum, maximum and average particle size determined based on the previous study.^{29,42} All the large particles are assumed to have evaporated into finite-size residual, and the value from the experiment is assumed to be the size of the residual particles.

To investigate the air cleaner placement effect, a $0.5 \times 0.5 \times 0.2$ m³ cuboid located 0.3 m above the ground is used to model the box fan air cleaner in the simulation [Fig. 3(c)]. The upper surface is the inlet of the air cleaner. The profile is set according to the measurements mentioned earlier. As shown in Fig. 3(a), two infector locations (i.e., locations A and B) and four air cleaner locations, i.e., in the front corner of the classroom (location 1), in the middle of the classroom near the HUV (location 2) and away from the HUV (location 3), and in the back of the classroom (location 4), in total eight cases are simulated. To study air cleaner flow direction effect, two additional cases, corresponding to two infector locations and the air cleaner placed in the middle of the classroom close to the HUV with the upward flow design (opposite to the previous cases) are included. For enhanced ventilation cases, the flow rate of the HUV is increased to achieve an increase in effective air changes from 2 ACH to 5 ACH with no air cleaner added in the simulation. To further examine the room size effect, we simulate cases using a computational domain of $10 \times 10 \times 3$ m³, which doubles the size of other cases. In this simulation, the flow rate of the HUV is also doubled to maintain an air exchange rate of 2 ACH for better comparison. Finally, in the cases studying the thermal effect, a $1.75 \times 0.5 \times 0.25$ m³ cuboid is used to represent a simplified thermal manikin. The surface of the manikin is set to be 30 °C, the respiratory flow is set to be 34 °C,⁴³ while the temperature of the HUV flow is 44 °C.⁴⁴ The flow rate of the respiratory flow is 2×10^{-4} m³/s based on experiment data²⁹ for all the simulation cases.

To characterize the risk of encountering virus-containing particles at a given location, we use the risk index introduced by Shao *et al.*,²⁹ denoted as I_{risk} . It is the total number of particles passing through a given location throughout the duration of the simulation and can be formulated as function of spatial location \mathbf{x} below,

$$I_{\text{risk}}(\mathbf{x}) = \sum P_i(\mathbf{x}),$$

where P_i is defined as

$$P_i(\mathbf{x}) = \begin{cases} 1, & \text{the first time the } i\text{th particle appears in a volume} \\ & \Delta V_B \text{ centered at location } \mathbf{x}, \\ 0, & \text{otherwise.} \end{cases}$$

Evidently, the choice of ΔV_B influences the absolute values of I_{risk} . Here we choose ΔV_B to be $2 \times 2 \times 2$ cm³, approximating the breathing zone characterized in the schlieren imaging experiments conducted in Shao *et al.*²⁹ It is worth noting that the breathing zone and corresponding ΔV_B can vary substantially under different breathing conditions and across different individuals, influence the absolute

TABLE I. A summary of all the simulation case setups and the corresponding particle (aerosol) distribution after a 50-min simulation period. Note that the particle distribution includes the percentages of particles extracted by air cleaners, by the horizontal unit ventilator (HUV), suspended in the air, and deposit on the wall after 50-min simulation.

		Infector location	Air cleaner location	Aerosol distribution after a 50-min simulation				
				Extracted by air cleaner	Extracted by ventilation (%)	Suspended (%)	Deposit on the wall (%)	
Baseline	Case A	A	NA	NA	5	15	80	
	Case B	B	NA	NA	8	13	79	
Placement effect	Case A1	A	1	43%	3	3	51	
	Case A2	A	2	41%	4	7	48	
	Case A3	A	3	19%	6	9	66	
	Case A4	A	4	14%	5	12	69	
	Case B1	B	1	24%	2	10	64	
	Case B2	B	2	75%	2	1	22	
	Case B3	B	3	27%	6	7	60	
	Case B4	B	4	24%	6	7	63	
	Case A12	A	1 and 2	53%	1	2	44	
	Case B12	B	1 and 2	84%	2	1	13	
	Flow direction	Case FA2	A	2 ^a	24%	4	6	66
		Case FB2	B	2 ^a	16%	3	8	73
Ventilation effect	Case VA	A	NA	NA	5	12	83	
	Case VB	B	NA	NA	8	12	80	
Room size effect	Case LB	B	NA	NA	11	14	75	
	Case LB2	B	2	20%	10	8	62	
	Case LB22	B	2 and 2	35%	5	8	52	
	Case LB12	B	1 and 2	28%	12	6	54	
Thermal effect	Case TA2	A	2	41%	3	9	41	
	Case TB2	B	2	65%	1	4	30	
	Case TA2H	A	2 ^b	26%	3	10	61	
	Case TB2H	B	2 ^b	78%	1	1	20	

^aRepresents the air cleaner with upward flow design.

^bRepresents placing the air cleaner 1.3 m above the ground.

values of I_{risk} . Therefore, we mainly rely on the relative change in I_{risk} to evaluate the variation of airborne transmission risk under different conditions. In addition, the spatial averaged I_{risk} (i.e., \bar{I}_{risk}) along each direction (x , y , or z) is also introduced to represent the 3D distribution of I_{risk} in the space. Same as the literature,²⁹ most particles in the simulation are below $5 \mu\text{m}$. The particles with size below $5 \mu\text{m}$ typically have Stokes number much less than 1, thus yield sufficient traceability to follow the smallest scale turbulence resolved in the simulation. Furthermore, presented simulation work focuses on airborne transmission associated with small particles ($<5 \mu\text{m}$). Therefore, using the I_{risk} to quantify the risk level is accurate since the I_{risk} value is primarily influenced by the air flow in the space.

For all simulation cases, hex-core meshes generated from ICEM 18.0 are used. To determine proper mesh size for the simulation, we have conducted grid independence test for simulation case I using two mesh sizes (1.5×10^6 and 2.7×10^6 cells). Both the coarse and fine mesh yield a similar result. Therefore, we use 1.5×10^6 cells for the remaining simulation cases related to placement effect, flow direction effect, ventilation effect, and corresponding baseline with similar settings. For simulations investigating the room size effect, the total

numbers of meshes are doubled for the large computational domain to maintain the mesh resolution unchanged. For the study of thermal effect, the total number of meshes are increased to 3.2×10^6 to ensure sufficient resolution to resolve thermal plumes from the infectors. The grid resolution is uniformly 5 cm in all three dimensions in the majority portion of the computational domain. The resolution is increased to 1 cm near the horizontal unit ventilator and air cleaner as well as the location of particle injection. For the simulation cases that involve thermal effect, the resolution near the manikin surface is further increased to 0.5 cm. The choice of these grid resolutions is based on the grid independence test and experimental validation in our past studies³¹ to ensure successful capture of the desired flow behaviors. The typical computational time for a 1-h simulation is about one week using a high-performance computing (HPC) system with 256 cores.

III. RESULTS

In this section, we will present the results of simulation cases showing the effects of placement and flow direction of box fan air cleaner on the particle removal and the corresponding distribution of airborne infection risk under the simulated classroom settings.

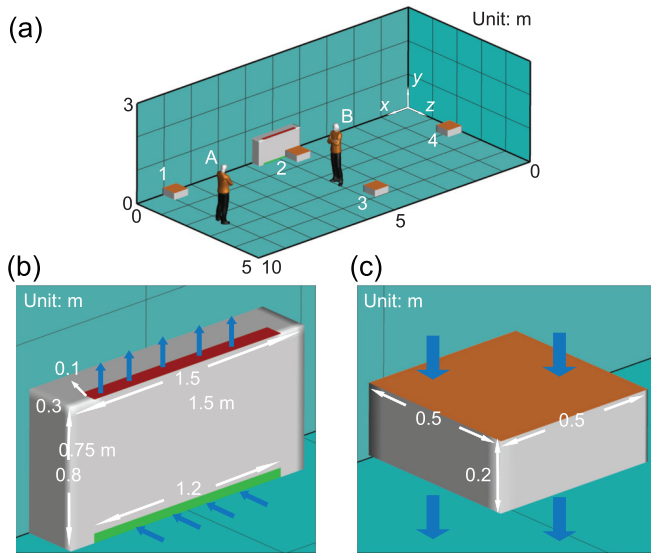


FIG. 3. Schematics showing (a) the computational domain and locations of infectors and box fan air cleaners in the classroom, (b) the setup of horizontal unit ventilator (HUV), and (c) the model of box fan air cleaner used in the simulation.

Moreover, we will further evaluate the performance of our air cleaner for airborne risk mitigation through a comparison with the simulation cases using only enhanced ventilation (no air cleaner placed in the room). Finally, we will investigate the influence of larger room size and the inclusion of thermal effects on our simulation results. The results including the percentages of particles extracted by the air cleaner and HUV, suspended particles in the air, and deposit on the surface after 50-min simulation are summarized in Table I.

A. Air cleaner placement effect

The effect of the placement of the box fan air cleaner on the particle extraction and the corresponding spatial variation of airborne transmission risk in the classroom is first investigated to determine the optimal placement location under the current settings. When the infector is in the front of the classroom (Fig. 4), the simulation case with no air cleaner [Fig. 4(a), served as the baseline] shows aerosols spread across the entire classroom, indicated by the region of $\bar{I}_{risk} \geq 1$ (green contour, defined as high-risk regions) extending all the way to the back of the classroom. Correspondingly, at the breathing level, the high-risk region (defined as $I_{risk} \geq 10$, green contour) covers beyond the half of the classroom. Note that the high-risk regions here are defined in a relative sense and this definition is used consistently for all the simulations cases present in the current study. As mentioned earlier, the absolute values of I_{risk} can be influenced by the definition of breathing zones and its value is only used for comparison across different cases.

When an air cleaner is placed near the infector [Fig. 4(b)], the spread of aerosols is almost confined to half of the classroom (i.e., the region corresponds to $\bar{I}_{risk} \geq 1$). Accordingly, at the breathing level, the high-risk region is limited to an area of ~ 1 m around the infector. In comparison, with the air cleaner moving near the HUV in the middle of the classroom [Fig. 4(c)], although its performance in terms of

lowering \bar{I}_{risk} and I_{risk} at the breathing level is reduced, but there is still considerable decrease in \bar{I}_{risk} and I_{risk} compared with the baseline case. When the air cleaner is shifted away from the HUV in the middle [Fig. 4(d)], the performance of the air cleaner further drops, with an enlarged area of high-risk region in both \bar{I}_{risk} and I_{risk} maps. Finally, placing the air cleaner in the back of the classroom [Fig. 4(e)] shows the lowest performance in suppressing \bar{I}_{risk} and I_{risk} , potentially due to the air cleaner locating farther from both the infector and HUV compared with all the other air cleaner simulation cases. Correspondingly, similar trends are observed in terms of percentages of aerosols extracted by the air cleaner and suspended aerosols among all the simulation cases with different air cleaner placements (Table I). Specifically, when the air cleaner is placed close to the infector, it extracts 43% aerosols with only 3% suspended in the air after a 50-min run, in comparison with the 15% suspended aerosols in the baseline case. Moving the air cleaner near the HUV maintains the same level of air cleaner extraction rate with 7% aerosols suspended. For the other two placement locations, the air cleaner extraction rate drops below 20% but the percentages of suspended aerosols are still lower than the baseline case. For all the simulation cases, a large fraction ($\geq 50\%$) of aerosols are found to deposit on surfaces after 50 min.

When the infector is placed in the middle of the classroom (Fig. 5), in comparison with the corresponding simulation case (case A) in Fig. 4, the baseline case shows a reduction of aerosol spread [Fig. 5(a)] and a decrease in the percentage of suspended aerosols (i.e., from 15% in case A to 13% in case B) and an increase in aerosols extracted by the HUV (i.e., from 5% in case A to 8% in case B), potentially associated with the infector being closer to the HUV. Similarly, due to the relocation of the infector, the location where the air cleaner has the best performance is shifted (from case A1) to the middle near the HUV (case B2). At this location, owing to its proximity to both the infector and HUV, the air cleaner can extract 75% of aerosols and leave only 1% aerosols suspended after 50 min (Table I), and correspondingly limit the high-risk regions to ~ 1 m around the infector [Fig. 5(c)]. Remarkably, as the air cleaner is moved away from the HUV but remains in the proximity of the infector (case B3), its performance drops significantly with the air cleaner extraction down to 25% and suspended percentage up to 7%, leading to wider spread of aerosols as shown in both \bar{I}_{risk} and I_{risk} maps at the breathing level [Fig. 5(d)]. The performance for the air cleaner located in the front [case B1, Fig. 5(b)] and back [case B4, Fig. 5(e)] of the classroom is similar but substantially lower compared to the two previous locations. Nevertheless, the risk levels for these two cases are still considerably lower than that for the baseline case [Fig. 5(a)], particularly in the vicinity of the infector.

Based on the above-mentioned investigation on air cleaner placement effect, it can be concluded that placing the air cleaner near the infector (i.e., cases A1 and B2) always yields the best performance. Comparing these two cases with their corresponding baseline cases [Figs. 6(a) and 6(d)], adding air cleaners can lower the I_{risk} at the breathing level across the entire classroom except near the areas very near (< 1 m) the infector or the air cleaner due to the directional flow induced by the air cleaner. However, when the infector location is not known, a more common scenario in practice, placing the air cleaner near the existing HUV is optimal. Specifically, averaging the aerosol distribution for the two infector locations (Figs. 4 and 5), the location close to the HUV in the middle yields the highest air cleaner extraction

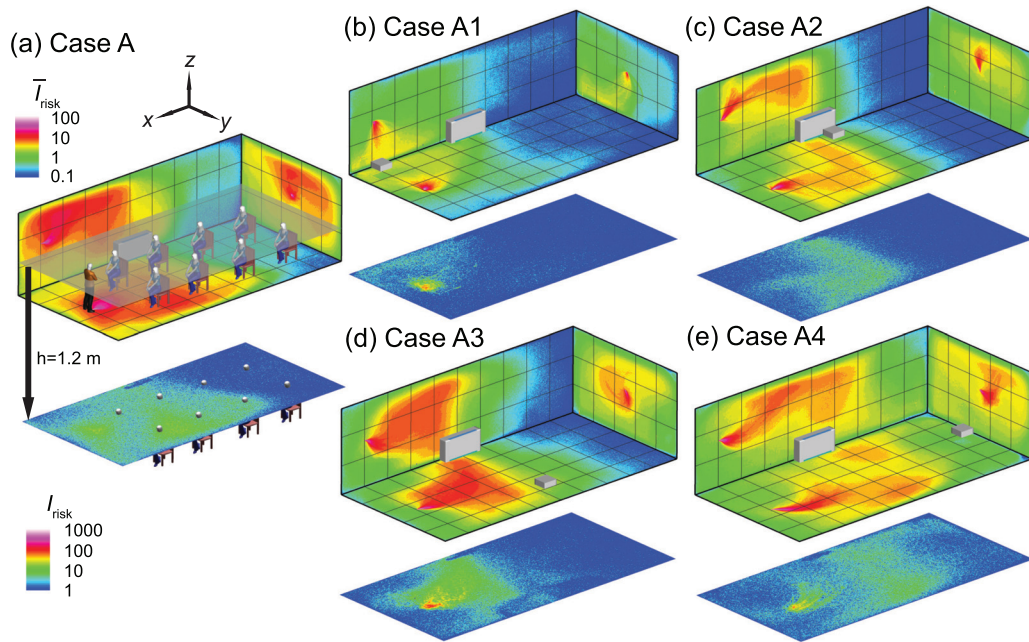


FIG. 4. The risk index (I_{risk}) maps of the classroom for an infector in the front of the classroom with (a) no box fan air cleaner placed (case A), (b) the air cleaner placed in the front of the classroom (case A1), (c) in the middle of the classroom near the horizontal unit ventilator (HUV) (case A2), (d) in the middle but away from the HUV (case A3), and (e) in the back of the classroom (case A4). The wall contour maps show the spatially averaged I_{risk} (\bar{I}_{risk}) along x, y, and z directions, respectively. The I_{risk} distribution at x-y plane at the breathing level of a sitting individual (1.2 m) is also provided. The contour of $\bar{I}_{risk} \geq 1$ and $I_{risk} \geq 10$ mark the regions of high-risk (relatively) in the space. The I_{risk} scales are consistent between different figure types but not between the two types: spatially averaged (top) and breathing level sections (bottom). Note that the human figures in (a) are used for illustration purposes and only the infector is modeled as a cuboid in the simulation.

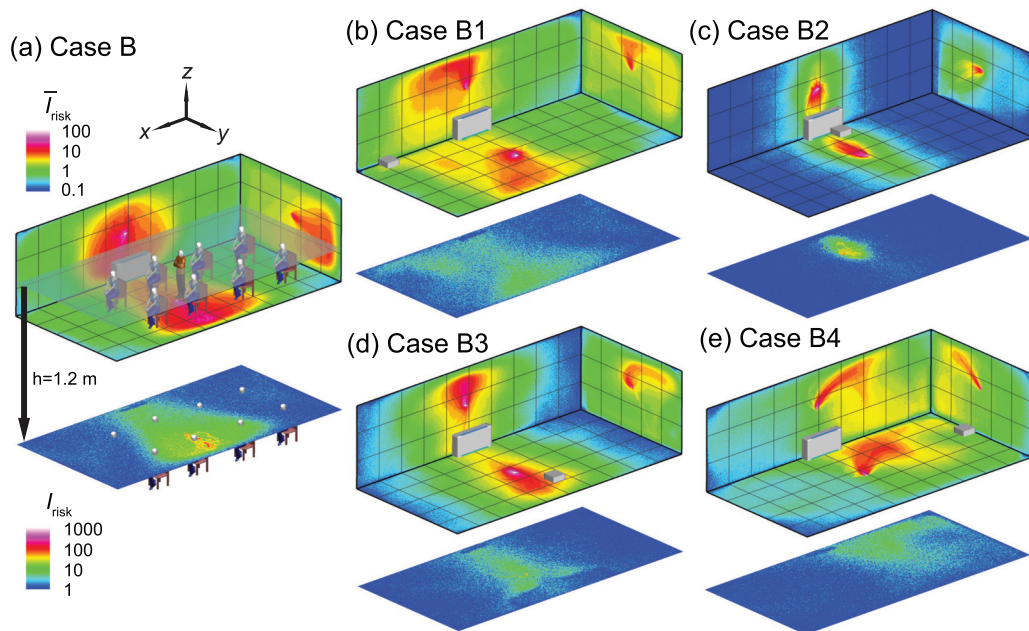


FIG. 5. The I_{risk} maps of the classroom for an infector in the middle of the classroom with (a) no box fan air cleaner placed (case B), (b) the air cleaner placed in the front (case B1), (c) in the middle of the classroom near the horizontal unit ventilator (HUV) (case B2), (d) in the middle but away from the HUV (case B3), and (e) in the back of the classroom (case B4). Note that the human figures in (a) are used for illustration purposes and only the infector is modeled as a cuboid in the simulation.

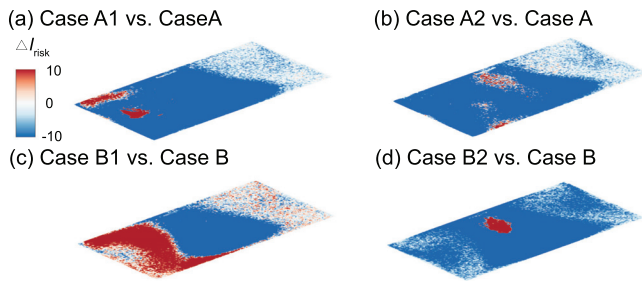


FIG. 6. Comparison of the I_{risk} map (ΔI_{risk}) at the breathing level for simulation cases with the air cleaner placed near the infector and near HUV, and the corresponding baseline case when the infector is in the front with the air cleaner placed (a) near the infector, or (b) near the HUV, and the infector is in the middle (b) with the air cleaner placed (c) near the infector, or (d) near the HUV. The ΔI_{risk} is defined as the I_{risk} of case A1 subtracted by that of case A for (a), case A2 subtracted by that of case A for (b), case B1 subtracted by that of case B for (c), and case B2 subtracted by that of case B for (d).

(58%) and lowest percentage of suspended aerosols (4%) among all four locations. Specifically, when the infector is in the front, placing the air cleaner near the HUV yields a decrease in high-risk region area across the room at the breathing level [Fig. 6(b)].

Furthermore, to elucidate the physical mechanism underlying the drastic performance drop of the air cleaner when its moves from near to away from the HUV (but remains in the proximity of the infector), we examine the flow field and aerosol deposition patterns for cases B2 and B3 in comparison to case B (Fig. 7). Without an air cleaner, the streamline pattern at the y - z middle plane (across the infector and the middle of HUV) exhibits a large circulation zone away from the HUV and adjacent to right sidewall [Fig. 7(a), highlighted by the red rectangle]. Such local circulation prolongs the pathways of aerosols moving toward the HUV [illustrated by the black dashed line in Fig. 7(a)] and hampers the extraction of aerosols by the ventilator. Instead, it increases aerosol residence time near the ceiling and right-sidewall, leading to a high percentage of aerosol deposition on these two walls. However, such circulation diminishes when the air cleaner is placed near the HUV [case B2, Fig. 7(b), highlighted by the red rectangle]. Instead, a large portion (about 70%) of the plane is dominated by downward flow toward the air cleaner and HUV [Fig. 7(b), highlighted by the yellow rectangle], which significantly shortens the pathway of aerosols being extracted [black dashed line in Fig. 7(b)] and lowers their residence time near the walls. Accordingly, aerosol deposition on the ceiling and right-sidewall is also largely reduced. In contrast, when the air cleaner is moved away from the HUV (case B3), the large local circulation zone reemerges with its center shifts closer to the ceiling [Fig. 7(c), highlighted by the red rectangle] in comparison to that in the baseline case [Fig. 7(a)]. In addition, a small circulation zone appears in the bottom right corner, associated with the interaction between the air cleaner induced flow field and the large circulation caused by the HUV. These circulations hinder the ability of aerosols being directly transported from the infector to the air cleaner [illustrated by the long and twisted black dashed line in Fig. 7(c)], lowering its performance drastically. These circulations also enhance the deposition of aerosols, particularly, on the right-sidewall near the air cleaner.

Simulations are also conducted to investigate the effectiveness of risk mitigation using multiple box fan air cleaners. Here we place one

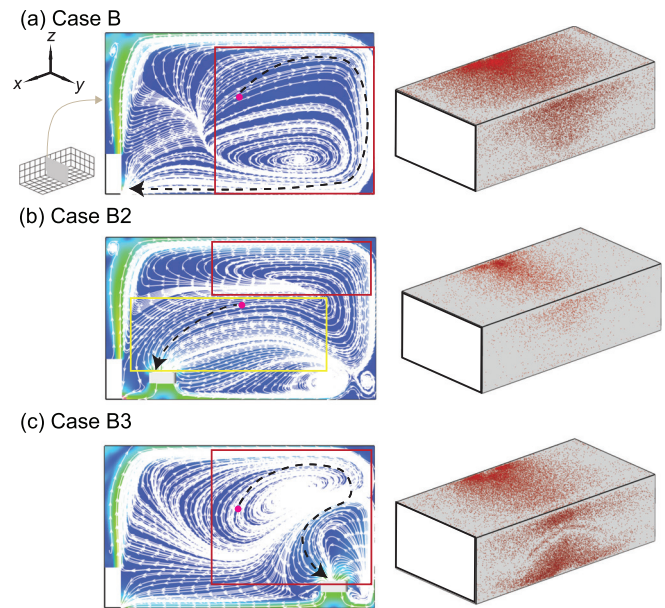


FIG. 7. Streamline flow map at the middle y - z plane (left) and aerosol wall deposition on the ceiling and right-side walls (right) for (a) case B, (b) case B2, and (c) case B3. The inset figure in (a) illustrating the positions of planes shown in the figures. The magenta dot represents the inject location and the black dashed lines in the streamline maps are used to illustrate potential pathways of the aerosols being extracted by the HUV or air cleaner.

air cleaner at each of the two locations (i.e., in the front and the middle of the classroom near the HUV) that yield the best performance among all the four locations examined above and simulate for the infector in the front [Fig. 8(a)] and the middle of the classroom [Fig. 8(b)]. For both cases, as shown in Fig. 9, the increase in the number of air cleaners can lead to further reduction of high-risk regions in the entire classroom (\bar{I}_{risk}) and at the breathing level (I_{risk}). Accordingly, when the infector is in the front, for the best air cleaner placement (i.e., case A1), adding an air cleaner near the HUV can increase the percentage of aerosols extracted by air cleaners from 43% to 53% and lower the suspended aerosols from 3% to 1% (i.e., case A1 vs case A12). When the infector is in the middle with an air cleaner near the HUV (i.e., case B2), the addition of an air cleaner to the front

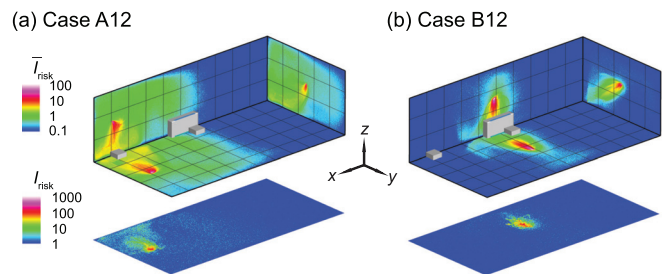


FIG. 8. The I_{risk} maps of the classroom with two box fan air cleaners for an infector (a) in the front (case A12) and (b) the middle (case B12) of the classroom. The two air cleaners are placed in the front and the middle near the HUV of the classroom, respectively.

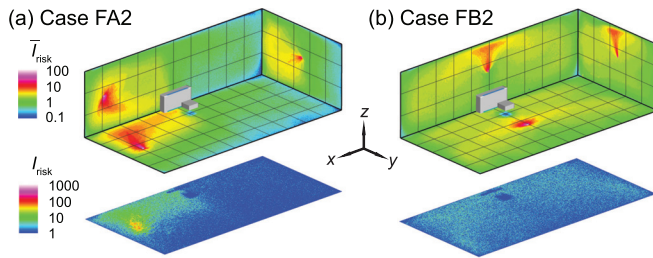


FIG. 9. The I_{risk} maps of the classroom with a flipped box fan air cleaner (i.e., upward flow design) for an infector (a) in the front (case FA2) and (b) the middle (case FB2) of the classroom.

increases the air cleaner extraction from 75% to 84% and but does not lead to appreciable change in the suspended particle percentage (i.e., case B2 vs case B12).

B. Air cleaner flow direction effect

The design of commercial air purifiers varies substantially across different manufacturers and models. Some of them uses an “upward flow” design, such as Molekule Air, Dyson Pure Cool TP04, and Honeywell HPA600B, in which the air cleaner sucks in contaminated air at the bottom while releasing clean air on the top. Others, including Oransi ERIK650A, employ a “downward flow” to gather polluted air on the top then discharge clean air from the bottom. Comparatively, for our box fan air cleaners, all the simulation cases presented above use the downward flow design. However, to evaluate the optimal flow direction for the box fan air cleaner, additional simulations are conducted using the upward flow design with the flow inlet surface facing downward. Based on the previous findings on air cleaner placement effect, only the optimal location, i.e., the location close to the HUV, is selected for this simulation.

In comparison to the downward flow design cases [Figs. 4(b) and 5(b)], upward flow design generally yields a decrease in performance. In particular, when the infector is in the middle near the air cleaner, the reverse of the flow direction leads to a substantial increase in aerosol spread, evidenced from the expansion of high-risk regions to the entire classroom at the breathing level [Fig. 9(b)]. Correspondingly, the suspended aerosols percentage increases from 1% to 8% with a steep drop of aerosols extracted by the air cleaner (from 75% to 16%). Such reduction in performance is manifested from the larger portion of red areas in the ΔI_{risk} maps at the breathing level [Fig. 10(b)]. In comparison, the performance drop is less severe when the infector is in the front of the classroom away from the air cleaner, and the

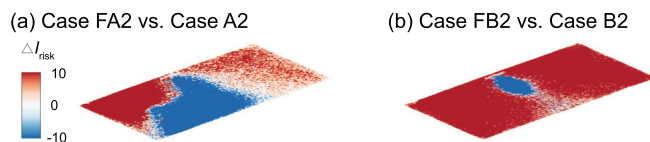


FIG. 10. Comparison of the I_{risk} map (ΔI_{risk}) at the breathing level between the downward and upward flow cases for the infector is (a) in the front and (b) in the middle of the classroom with the air cleaner located near the HUV. The ΔI_{risk} is defined as the I_{risk} of case FA2 subtracted by that of case A2 for (a) and the I_{risk} of case FB2 subtracted by that of case B2 for (b).

suspended aerosols stay close to the level of downward flow case. Nevertheless, a considerable decay in the aerosols extracted by the cleaner is observed (from 41% to 24%) with an elevated aerosol spread [Fig. 9(a)].

To elucidate the physical mechanism behind the significant performance reduction associated with the change of inflow direction, we investigate the flow field and aerosol deposition patterns for case FB2 in comparison with case B2. Specifically, when the flow design is upward, a large portion of the plane is governed by upward flow away from the HUV and the air cleaner (Fig. 11, highlighted by the red rectangle) instead of dominated by the flow toward the HUV and the air cleaner in the downward design case [Fig. 7(b)]. Such flow field changes due to the flip of the flow direction significantly extend the pathway of aerosols being extracted (black dashed line in Fig. 11) and increase their residence time near the walls, leading to a significant increase in the aerosol deposition (from 22% to 73%). Correspondingly, aerosol deposition on the ceiling and right-side wall is increased as well (Fig. 11).

C. Enhanced ventilation effect

A common recommendation for risk mitigation in poorly ventilated spaces is to increase ventilation rate¹⁸ in order to achieve a higher effective air changes, typically to at least 5 ACH.¹⁸ Therefore, additional simulations are conducted to evaluate the performance of enhanced ventilation in comparison with that of placing box fan air cleaners. Here we simulate a classroom with ventilation enhanced to 5 ACH but no air cleaner for the infector in the front [case VA, Fig. 13(a)] and in the middle [case VB, Fig. 13(b)]. Compared with the baseline cases at lower ventilation of 2 ACH (Fig. 4), ventilation enhancement can lead to reduction in the high-risk regions (Fig. 12) and suspended aerosol percentage (from 15% to 8% for the infector in the front, and from 12% to 7% for the infector in the middle). However, in comparison to the optimally placed air cleaner solution (cases A1 and B2), the performance of enhanced ventilation is significantly lower. Such discrepancy is evidenced from the larger portion of red areas in the ΔI_{risk} maps at the breathing level (Fig. 13), which indicates an increase in risk level when enhanced ventilation case is compared with its corresponding air cleaner case. Accordingly, the air cleaner solutions yield much lower suspended aerosols (3% for case A1 and 1% for case B2) vs those for enhanced ventilation cases (8% for case VA and 7% for case VB). Such comparison suggests that using local air cleaners placed near the infector or ventilator is a more

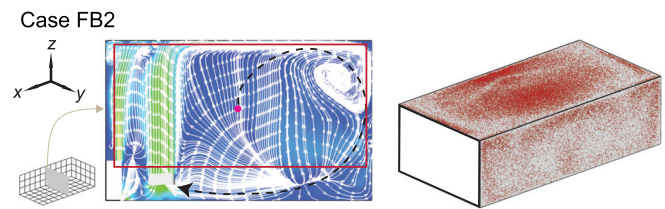


FIG. 11. Streamline flow map at the middle y - z plane (left) and aerosol wall deposition on the ceiling and right-side walls (right) for case FB2. The magenta dot represents the inject location and the black dashed lines in the streamline maps are used to illustrate potential pathways of the aerosols being extracted by the HUV or air cleaner.

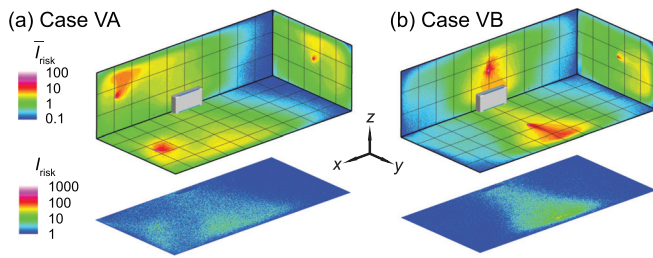


FIG. 12. The I_{risk} maps of the classroom with enhanced ventilation (5 ACH) for an infector (a) in the front (case VA) and (b) the middle (case VB) of the classroom.

effective approach for risk mitigation than simply enhancing the flow rate of a single ventilation unit.

D. Room size effect

In this section, we investigate the effect of classroom size on the performance of box fan air cleaners for risk mitigation since classrooms with various sizes are present in practice. Here, we simulate a classroom with double the size of that used in previous simulations, i.e., $10 \times 10 \times 3 \text{ m}^3$ (vs $10 \times 5 \times 3 \text{ m}^3$ used earlier), matching one of the common classroom sizes used in the United States. In these simulations, the air cleaner is placed at its optimal location (near the HUV) for the infector in the middle. Even without changing the flow rate in a double-sized classroom, the air cleaner can still reduce the regions of high risk, particularly at the breathing level [Fig. 14(b)], and suspended aerosol percentage (8%), in comparison to the case without air cleaners [Fig. 14(a) and 14% suspended aerosols]. However, compared with the corresponding smaller classroom case (case B2) which only yields 1% suspended aerosols, the performance of air cleaner drops with increasing room size.

Subsequently, to further reduce aerosol spread with increasing room size, we use simulations to examine and compare the effectiveness of two approaches, i.e., increasing air cleaner flow rate and adding more air cleaners. Specifically, two simulation cases are investigated for the infector in the middle, i.e., one that doubles the flow rate of air cleaner near the HUV and the other that adds an air cleaner in the front. Remarkably, doubling the air cleaner flow rate does not lead to appreciable reduction in suspended aerosol percentage (still 8%), but in contrast (compared with the lower rate) causes more spread of aerosols at the breathing level [Fig. 15(a)] compared with the corresponding lower flow rate case [Fig. 15(b)]. In contrast, placing two air cleaners at lower flow rate can reduce high-risk regions at the breathing level [Fig. 15(b)] and lower the suspended aerosols (from 8% to

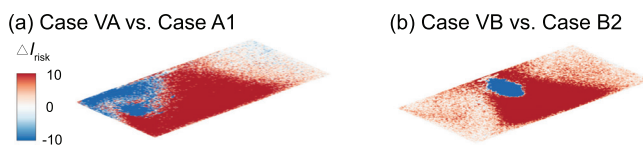


FIG. 13. Comparison of the I_{risk} map (ΔI_{risk}) at the breathing level between the enhanced ventilation and optimal placement cases for the infector (a) in the front and (b) in the middle of the classroom with the air cleaner located near the HUV. The ΔI_{risk} is defined as the I_{risk} of case VA subtracted by that of case A1 for (a) and the I_{risk} of Case VB subtracted by that of Case B2 for (b).

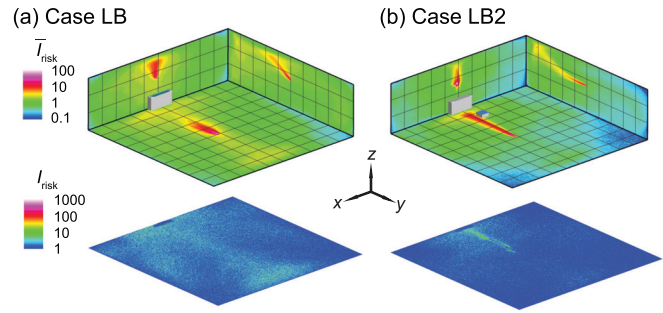


FIG. 14. The I_{risk} maps of the classroom for an infector in the middle of the classroom with (a) no box fan air cleaner placed (case LB served as a baseline) and (b) the air cleaner placed in the middle near the HUV (case LB2).

6%). This result suggests that it is more effective to distribute air cleaners to multiple locations than to simply increase the flow rate of a single air cleaner or ventilation unit for risk mitigation in large size rooms.

E. Thermal effect

As shown in the literature, the temperature difference among ventilation air, human surface temperature, and ambient room air can influence the spread of aerosols in indoor spaces. Particularly, the heated classrooms in winter and air-conditioned classrooms in summer may yield considerable temperature gradient which could lead to a thermal flow that is comparable to or more dominant than ventilation flow in, especially, poorly ventilated spaces. Therefore, we conduct the simulation under a simplified scenario representing a heated classroom in winter. When the thermal effect associated with human thermal plume and hot ventilation is included in the simulation, the performance of box fan air cleaners drops, manifested as an increase in high-risk regions in the \bar{I}_{risk} and I_{risk} maps [Fig. 16(a) vs Fig. 4(c) and Fig. 16(b) vs Fig. 5(c) for the infector in the front and in the middle of the classroom, respectively]. Such increase is illustrated more clearly in the ΔI_{risk} map at the breathing level, corresponding to the larger area of red contours in comparison to that of blue in Fig. 17. Correspondingly, with the inclusion of thermal effect, the suspended aerosol percentage increases from 7% to 9% and from 1% to 4% for the infector in the front and the middle, respectively. It is worth noting

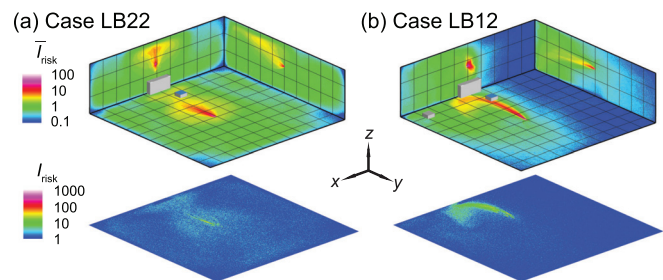


FIG. 15. The I_{risk} maps of the classroom for an infector in the middle of the classroom with (a) a single air cleaner placed near the HUV with double the flow rate of the previous simulation cases (case LB22), and (b) one air cleaner near the HUV and the other in the front (case LB12).

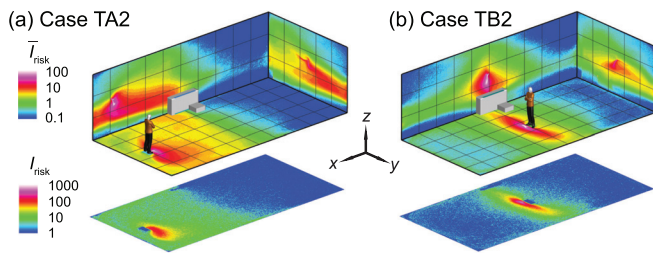


FIG. 16. The I_{risk} maps of the classroom when the thermal effect associated with human thermal plume and hot ventilation is considered for the infector (a) in the front (case TA2) and (b) the middle of the classroom with the air cleaner near the HUV (case TB2). Note that the human figures in (a) and (b) are used for illustration purposes. The infector is modeled as a cuboid in the simulation.

that the decrease in air cleaner performance is more substantial when the air cleaner is located farther away from the infector. We attribute such decrease to the change in flow patterns associated with thermal effect. Specifically, the flow induced by the thermal gradient causes the formation of large recirculation adjacent to the ceiling (Fig. 18, highlighted by the red rectangle). The aerosols produced by the infector tend to move upward due to the thermal plume and be trapped in this circulation thus have higher chance to deposit on the wall and disperse instead of directly transport toward the air cleaner (Fig. 18). Sample video of the particle transport simulation for case TB2 can be found in [supplementary material Video 2](#). Note that the human figures in the video are used for illustration purposes and only the infector is modeled as a cuboid in the simulation.

To explore whether the placement of air cleaners can be adjusted to achieve better performance under the influence of thermal gradient, we simulate additional cases in which the air cleaner is raised 1 m vertically from its original position, i.e., 1.3 m above the floor (Fig. 19). As shown in Figs. 19(b) and 20(b), a clear improvement in air cleaner performance is observed for the case with the infector in the middle and the air cleaner located in proximity of the infector. This improvement is because the elevating air cleaner can take advantage of human thermal plume to improve its particle extraction (changing from 65% to 78%) and decrease the spread of aerosol transmission [Fig. 20(b)]. However, when the infector is located farther away from the air cleaner [Fig. 19(a)], the performance of the air cleaner drops with elevated placement [indicated by the larger area of red contour than that of blue in Fig. 20(a)]. Such discrepancy in the performance of the elevated air cleaner between cases TA2H and TB2H is due to the fact that human thermal plume is only dominant in the vicinity of the infector and the elevated air

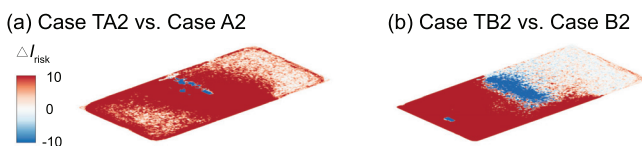


FIG. 17. Comparison of the I_{risk} map at the breathing level between the simulation cases with and without consideration of thermal effect for the infector (a) in the front and (b) in the middle of the classroom with the air cleaner near the HUV. The ΔI_{risk} is defined as the I_{risk} of case TA2 subtracted by that of case A2 for (a) and the I_{risk} of case TB2 subtracted by that of case B2 for (b).

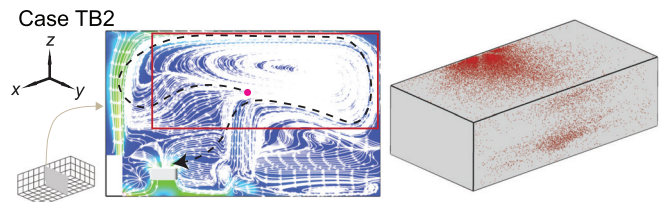


FIG. 18. Streamline flow map at the middle y - z plane (left) and aerosol wall deposition on the ceiling and right-side walls (right) for case TB2. The magenta dot represents the inject location and the black dashed lines in the streamline maps are used to illustrate potential pathways of the aerosols being extracted by the HUV or air cleaner.

cleaner located far away from the infector can no longer benefit from the aerosol transport by thermal updraft.

IV. CONCLUSION AND DISCUSSION

Using computational fluid dynamics, we provide a systematic investigation of airborne transmission in a poorly ventilated classroom and evaluate the performance of low-cost box fan air cleaners for risk mitigation. The classroom is modeled with a single horizontal unit ventilator (HUV) operating at an air exchange rate of ~ 2 ACH, representing the ventilation setting in a typical classroom built before 1989.³⁰ Our study shows that placing box fan air cleaners in the classroom results in a substantial reduction of airborne transmission risk across the entire space. The performance of the cleaner, in terms of its efficiency to extract aerosols and lower the percentage of suspended aerosols from potential infectors, is strongly influenced by its placement. We find that the cleaner can achieve best performance when placed near the infector. However, without knowing the location of the patient, the performance of the cleaner is optimal near the HUV. Specifically, at the optimal placement, the cleaner can extract the majority of aerosols emitted continuously from an asymptomatic instructor (infector) and reduce the suspended aerosols down to 1% after a 50-min simulation of a lecture, significantly lower than the condition without the cleaner (13%). In addition, the simulations show that the air cleaner with downward flow design (i.e., the flow inlet of the cleaner facing upward) performs better than the upward flow one, resulting in a more confined high-risk region and lower percentage of suspended aerosols when situated near the infector particularly.

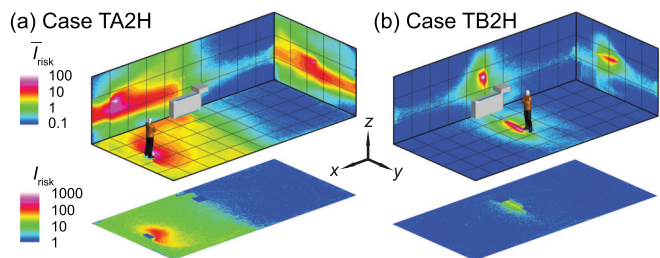


FIG. 19. The I_{risk} maps of the classroom when the thermal effect is considered with the air cleaner placed near the HUV at a higher elevation (1.3 m above the floor) compared with previous simulation cases (0.3 m above the floor) for an infector (a) in the front (case TA2H) and (b) in the middle (case TB2H) of the classroom. Note that the human figures in (a) and (b) are used for illustration purposes. The infector is modeled as a cuboid in the simulation.

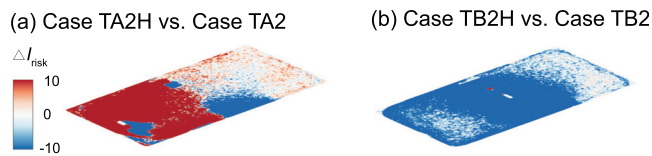


FIG. 20. Comparison of the I_{risk} map at the breathing level between the simulation cases with an air cleaner placed 1.3 m and 0.3 m above the floor near the HUV for the infector (a) in the front and (b) in the middle of the classroom. The ΔI_{risk} is defined as the I_{risk} of case TA2H subtracted by that of case TA2 for (a) and the I_{risk} of case TB2H subtracted by that of case TB2 for (b).

In comparison to raising the air exchange rate of the HUV (i.e., from 2 ACH to 5 ACH), the air cleaner solution can result in higher reduction in aerosol concentration and spread in the classroom. As the classroom size increases, with placement of additional cleaners separately in the domain, the air cleaner solution can still lead to a confined dispersion of aerosols and a significant reduction of the suspended aerosols. In contrast, doubling the cleaner flow rate to accommodate increasing room size may cause even more spread of aerosols at the breathing level compared with the cleaner operating at lower flow rate. When considering the thermal gradient associated with the human thermal plume and hot ventilation air during cold seasons, the overall performance of air cleaners drops but their efficacy in reducing aerosol spread and regions of high-risk airborne transmission still holds compared with the baseline case with only ventilation. We also find that elevating the cleaner when it is placed near an infector can increase its performance by taking advantage of human thermal plumes that drive particles moving upward.

Our work has demonstrated the various effects of implementing air cleaners in a poorly ventilated classroom that relies on a horizontal unit ventilator (HUV). The methodology and the results from our study are generally applicable for evaluating of efficacy of the air cleaner solution for other poorly ventilated spaces including aged offices, prisons, homeless shelters, etc. One of the insights of the CFD analysis is that the air cleaner can not only reduce the overall concentration of aerosols in the space but also limit the spread. These results could conceivably be applied to other types of portable air filtration systems. A novel aspect of this study, compared to previous portable air filtration system studies, is that it does not look at a “well mixed,” more uniform distribution across the space. Instead, it explores the implications of placing portable air cleaners in a representative space as it is likely done in practice.

According to our results, placing the air cleaner next to the infector is the most effective. If the individuals (if they are asymptomatic infectors) who can impose the highest risk to others can be identified in space, air cleaners should be placed in the proximity of these individuals to limit the spread of their emitted aerosols. In practical settings (e.g., classroom, concert, etc.), it is better to take the precaution to place air cleaners near unmasked teachers, singers, and trumpet players who can produce a large number of aerosols during their activities or a new person entering a relatively quarantined group. However, when such high-risk individuals and their locations cannot be identified beforehand, the best practice is to place the air cleaner near the existing ventilation system. Under such placement, air cleaner is acting as a high specification filter for the unit ventilator. It is shown from the simulation that the convection flow is enhanced when

placing the air cleaner close to the existing ventilation system, thus minimizing the recirculation zone in the space and allowing more aerosols to be entrained in the main circulation path and removed by the air cleaner. Unit ventilators are performing the job of conditioning the air and providing fresh oxygen to the room. However, many of them are not designed to take a high specification filter. By implementing the air cleaner near the existing ventilation system, the air available to the unit ventilator is filtered as to add this capability to the system. This allows the unit ventilator to continue conditioning and mixing the air without losing performance and disrupting the circulation of the room.

Two air cleaners in the room can capture a large portion of the emitted aerosols from the infector directly into the air cleaners. There is a localized high-risk region close to the infector, but the rest of the space has low risks. Our results suggest that multiple air cleaners could be used to locally target and remove aerosols and limit their spread across the room. Although such deployment depends on the available resources and the type of HVAC system that is being utilized, it is a definite advantage of the low-cost box fan air cleaner as it could allow multiple deployments in a space for the same or fraction of the price as one expensive commercial air purifier when properly weighted against other factors such as noise.

It is worth noting that all the cases are simulated with an aerosol emission rate corresponding to unmasked individuals. Considering wearing mask in closed spaces such as classrooms is a suggested method which can potentially lower the aerosol emission, it is conceivable that the risk levels under masked conditions are substantially lower than those in our simulated cases. Nevertheless, we expect the spatial distribution of risk regions reported in our study will not be largely influenced by the presence of masks since the mask only affect the flow field very near the infector and the transport of aerosols in the space is dominated by the flows generated from the ventilation and cleaners. In addition, it is worth noting that wearing mask can hamper voice directivity and speech intelligibility,⁴⁵ imposing a detrimental impact on learning, particularly in large classrooms or for hearing impaired learners. As an alternative solution, placing the air cleaner close to the instructor can substantially mitigate the transmission risk without compromising on teaching quality.

There are many variables that affect specific details of airflow, ventilation, and aerosol dynamics in a particular space. Our results only provide general trends and should not be treated as absolute criteria for a specific environment. For example, the particle-wall interaction model relies on commonly used assumptions.⁴⁶ Its validity on aerosol size particles relevant to disease transmission has not been fully examined, which may impose an uncertainty on the aerosol percentage present in our study. Nevertheless, the comparison in the relative percent reduction between different cases is valuable information. The thermal effects are examined in a simplified classroom setting which demonstrates that the addition of thermal plumes does not change the effectiveness of the system. However, our simulation uses a simplistic environment with uniform wall conditions and very few loads in the space (e.g., people and equipment). These simplifications may cause some difference in the flow patterns (e.g., the upper circulation zone) between our simulation and real settings. Nevertheless, the comparison of our results (thermal cases) with nonthermal cases indicates that the efficacy of our cleaners for risk mitigation remains reasonable robust against the change of flow patterns associated with thermal effect.

Our findings can also help guide the implementation of air cleaners for risk mitigation in other indoor poorly ventilated spaces including prisons, downmarket offices, homeless shelters, life care centers, etc. Specifically, for example, homeless shelters commonly use a central HVAC system equipped with low-efficiency filters (i.e., MERV 8 or below)⁴⁷ at the ceiling and have an outside air supply that is below ASHRAE's standard (i.e., 15 cfm per person).⁴⁸ To mitigate airborne transmission risks in these places, we can place our air cleaner below the air return location in the room to serve as a low-cost booster of their central HVAC system with improved flow rate and filtration efficiency. For large size shelters, we propose to use multiple air cleaners (owing to their low cost) distributed in the space and placed near the potential sources of emission for optimal risk mitigation.

Correlating the modeled aerosol concentration and distribution over time to field and laboratory measurements will be important to validate the parameters and boundary conditions used in this study. In addition, a follow-up study involving a systematic comparison between experiments and CFD can help provide a deeper understanding of how well CFD modeling tools can reliably assess concentration and risk, especially for unique boundary conditions, complex thermal effects, aerosol counts, and use cases not directly addressed in this study.

SUPPLEMENTARY MATERIAL

See the [supplementary material](#) for the sample video showing the interaction between the particle and the flow of the box fan air cleaner (Supplementary Video1) and the sample video showing the simulated particles for case TB2 (Supplementary Video2).

ACKNOWLEDGMENTS

We acknowledge the support from Ford Motor Company for this research. We would like to thank Dr. Siyao Shao and Mr. Rafael Grazzini Placucci for conducting the flow visualization experiment. In addition, we also would like to acknowledge the support from Minnesota Supercomputing Institute (MSI) that provides computational resources.

DATA AVAILABILITY

The data that support the findings of this study are available from the corresponding author upon reasonable request.

REFERENCES

- L. Morawska and J. Cao, "Airborne transmission of SARS-CoV-2: The world should face the reality," *Environ. Int.* **139**, 105730 (2020).
- J. A. Lednický, M. Lazard, Z. H. Fan, A. Jutla, T. B. Tilly, M. Gangwar, M. Usmani, S. N. Shankar, K. Mohamed, A. Eiguren-Fernandez, C. J. Stephenson, M. M. Alam, M. A. Elbadry, J. C. Loeb, K. Subramaniam, T. B. Waltzek, K. Cherabuddi, J. G. Morris, and C. Y. Wu, "Viable SARS-CoV-2 in the air of a hospital room with COVID-19 patients," *Int. J. Infect. Dis.* **100**, 476–482 (2020).
- J. Lu, J. Gu, K. Li, C. Xu, W. Su, Z. Lai, D. Zhou, C. Yu, B. Xu, and Z. Yang, "COVID-19 outbreak associated with air conditioning in restaurant, Guangzhou, China, 2020," *Emerging Infect. Dis.* **26**(7), 1628 (2020).
- J. L. Santarpia, D. N. Rivera, V. L. Herrera, M. J. Morwitzer, H. M. Creager, G. W. Santarpia, K. K. Crown, D. M. Brett-Major, E. R. Schnaubelt, M. J. Broadhurst, J. v. Lawler, S. P. Reid, and J. J. Lowe, "Aerosol and surface contamination of SARS-CoV-2 observed in quarantine and isolation care," *Sci. Rep.* **10**, 1–8 (2020).
- S. Y. Park, Y. M. Kim, S. Yi, S. Lee, B. J. Na, C. B. Kim, J. il Kim, H. S. Kim, Y. B. Kim, Y. Park, I. S. Huh, H. K. Kim, H. J. Yoon, H. Jang, K. Kim, Y. Chang, I. Kim, H. Lee, J. Gwack, S. S. Kim, M. Kim, S. Kweon, Y. J. Choe, O. Park, Y. J. Park, and E. K. Jeong, "Coronavirus disease outbreak in call center, South Korea," *Emerging Infect. Dis.* **26**(8), 1666 (2020).
- S. L. Miller, W. W. Nazaroff, J. L. Jimenez, A. Boerstra, G. Buonanno, S. J. Dancer, and C. Noakes, "Transmission of SARS-CoV-2 by inhalation of respiratory aerosol in the Skagit Valley Chorale superspreading event," *Indoor Air* **31**(2), 314–323 (2021).
- Y. Shen, C. Li, H. Dong, Z. Wang, L. Martinez, Z. Sun, A. Handel, Z. Chen, E. Chen, M. H. Ebell, F. Wang, B. Yi, H. Wang, X. Wang, A. Wang, B. Chen, Y. Qi, L. Liang, Y. Li, F. Ling, J. Chen, and G. Xu, "Community outbreak investigation of SARS-CoV-2 transmission among bus riders in Eastern China," *JAMA Intern. Med.* **180**(12), 1665–1671 (2020).
- ASHRAE, "Pandemic COVID-19 and airborne transmission" (2020).
- L. Morawska, J. W. Tang, W. Bahnfleth, P. M. Bluyssen, A. Boerstra, G. Buonanno, J. Cao, S. Dancer, A. Floto, F. Franchimon, C. Haworth, J. Hogeling, C. Isaxon, J. L. Jimenez, J. Kurnitski, Y. Li, M. Loomans, G. Marks, L. C. Marr, L. Mazzarella, A. K. Melikov, S. Miller, D. K. Milton, W. Nazaroff, P. v. Nielsen, C. Noakes, J. Peccia, X. Querol, C. Sekhar, O. Seppänen, S. ichi Tanabe, R. Tellier, K. W. Tham, P. Wargocki, A. Wierzbicka, and M. Yao, "How can airborne transmission of COVID-19 indoors be minimized?," *Environ. Int.* **142**, 105832 (2020).
- A. K. Melikov, "Advanced air distribution: Improving health and comfort while reducing energy use," *Indoor Air* **26**(1), 112–124 (2016).
- J. M. Nowicki, "K-12 education: School districts frequently identified multiple building systems needing updates or replacement," Report No. GAO-20-494 (US Government Accountability Office, 2020).
- W. R. Chan, X. Li, B. C. Singer, T. Pistochini, D. Vernon, S. Outcalt, A. Sanguinetti, and M. Modera, "Ventilation rates in California classrooms: Why many recent HVAC retrofits are not delivering sufficient ventilation," *Build. Environ.* **167**, 106426 (2020).
- J. Adelman, "Fresh air will be a hot amenity in reopened offices if companies can afford it," Philadelphia Enquirer, (May 25, 2020), <https://www.inquirer.com/business/coronavirus-offices-hvac-philadelphia-rent-covid-ventilation-filtration-old-buildings-20200525.html>
- H. Qian, Y. Li, W. H. Seto, P. Ching, W. H. Ching, and H. Q. Sun, "Natural ventilation for reducing airborne infection in hospitals," *Build. Environ.* **45**(3), 559–565 (2010).
- See <https://www.cdc.gov/coronavirus/2019-ncov/community/ventilation.html> for "Ventilation in buildings," Centers for Disease Control and Prevention (CDC) (2021).
- R. J. Shaughnessy and R. G. Sextro, "What is an effective portable air cleaning device? A review," *J. Occup. Environ. Hyg.* **3**(4), 169–181 (2006).
- J. Curtius, M. Granzin, and J. Schrod, "Testing mobile air purifiers in a school classroom: Reducing the airborne transmission risk for SARS-CoV-2," *Aerosol Science and Technology* 1–14 (2021).
- J. Allen, J. Spengler, E. Jones, and J. Cedeno-Laurent, "5-step guide to checking ventilation rates in classrooms," Harvard Healthy Buildings Program (2020), see https://schools.forhealth.org/wp-content/uploads/sites/19/2021/01/Harvard-Healthy-Buildings-program-How-to-assess-classroom-ventilation-10-30-2020-EN_R1.8.pdf
- S. Kirkman, J. Zhai, and S. L. Miller, "Effectiveness of air cleaners for removal of virus-containing respiratory droplets: Recommendations for air cleaner selection for campus spaces" (2020), see <https://shellym80304.files.wordpress.com/2020/06/air-cleaner-report.pdf>
- A. Tseng, "DIY air filters can be safe, simple and inexpensive. Here's how to make one," LA Times (2020), see <https://www.latimes.com/environment/story/2020-09-17/best-air-filters-sold-out-how-to-make-diy-purifier>
- H. Liu, S. He, L. Shen, and J. Hong, "Simulation-based study of COVID-19 outbreak associated with air-conditioning in a restaurant," *Phys. Fluids* **33**(2), 023301 (2021).
- M.-R. Pendar and J. C. Páscoa, "Numerical modeling of the distribution of virus carrying saliva droplets during sneeze and cough," *Phys. Fluids* **32**(8), 083305 (2020).
- Z. Li, H. Wang, X. Zhang, T. Wu, and X. Yang, "Effects of space sizes on the dispersion of cough-generated droplets from a walking person," *Phys. Fluids* **32**(12), 121705 (2020).

- ²⁴J. Xi, X. A. Si, and R. Nagarajan, "Effects of mask-wearing on the inhalability and deposition of airborne SARS-CoV-2 aerosols in human upper airway," *Phys. Fluids* **32**(12), 123312 (2020).
- ²⁵A. Foster and M. Kinzel, "Estimating COVID-19 exposure in a classroom setting: A comparison between mathematical and numerical models," *Phys. Fluids* **33**(2), 021904 (2021).
- ²⁶Z. Lin, J. Wang, T. Yao, T. T. Chow, and K. F. Fong, "Numerical comparison of dispersion of human exhaled droplets under different ventilation methods," *World Rev. Sci. Technol. Sustainable Dev.* **10**, 142–161 (2013).
- ²⁷Y. Zhang, G. Feng, K. Huang, and G. Cao, "Numerical simulation of aerosol particles distribution in a classroom," in Proceedings of the 8th International Symposium on Heating, Ventilation and Air Conditioning (2014), pp. 203–210.
- ²⁸M. Abuhegazy, K. Talaat, O. Anderoglu, S. v. Poroseva, and K. Talaat, "Numerical investigation of aerosol transport in a classroom with relevance to COVID-19," *Phys. Fluids* **32**(10), 103311 (2020).
- ²⁹S. Shao, D. Zhou, R. He, J. Li, S. Zou, K. Mallery, S. Kumar, S. Yang, and J. Hong, "Risk assessment of airborne transmission of COVID-19 by asymptomatic individuals under different practical settings," *J. Aerosol Sci.* **151**, 105661 (2021).
- ³⁰School HVAC Design Manual, DAIKIN (2014).
- ³¹A. Abraham, R. He, S. Shao, S. Santosh Kumar, C. Wang, B. Guo, M. Trifonov, R. Grazzini Placucci, M. Willis, and J. Hong, "Risk assessment and mitigation of airborne disease transmission in orchestral wind instrument performance," *J. Aerosol Sci.* (2021).
- ³²S. R. Narayanan and S. Yang, "Airborne transmission of virus-laden aerosols inside a music classroom: Effects of portable purifiers and aerosol injection rates," *Phys. Fluids* **33**, 033307 (2021).
- ³³See <https://advocate.socialchorus.com/ford/blueovalnow/articles/how-to-assemble-a-covid-19-air-filtration-box-fan?5d08ebff=fa2a1297> for How to Assemble a COVID-19 Air Filtration Box Fan.
- ³⁴ASHRAE Standing Standard Project, "Method of testing general ventilation air-cleaning devices for removal efficiency by particle size" (2017).
- ³⁵ANSI/AHAM AC-1–2019, Association of Home Appliance Manufacturers (2019).
- ³⁶A. Nazari, M. Jafari, N. Rezaei, F. Taghizadeh-Hesary, and F. Taghizadeh-Hesary, "Jet fans in the underground car parking areas and virus transmission," *Phys. Fluids* **33**(1), 013603 (2021).
- ³⁷D. N. Sørensen and P. v. Nielsen, "Quality control of computational fluid dynamics in indoor environments," *Indoor Air* **13**(1), 2–17 (2003).
- ³⁸A. Hasan, "Tracking the flu virus in a room mechanical ventilation using CFD tools and effective disinfection of an HVAC system," *Int. J. Air-Cond. Refrig.* **28**(2), 2050019 (2020).
- ³⁹H. Zhang, D. Li, L. Xie, and Y. Xiao, "Documentary research of human respiratory droplet characteristics," *Procedia Eng.* **121**, 1365–1374 (2015).
- ⁴⁰M. Vaish, "Lung-aerosol dynamics in human airway models: Validation and application of OpenFOAM software" (2014).
- ⁴¹J. Q. Feng, "A computational study of particle deposition patterns from a circular laminar jet," *J. Appl. Fluid Mech.* **10**(4), 1001–1012 (2017).
- ⁴²S. Asadi, A. S. Wexler, C. D. Cappa, S. Barreda, N. M. Bouvier, and W. D. Ristenpart, "Aerosol emission and superemission during human speech increase with voice loudness," *Sci. Rep.* **9**(1), 1–10 (2019).
- ⁴³Valedictorian* - Vertical Unit Ventilator Models VFF and VFV, MODINE (2012).
- ⁴⁴J. K. Gupta, C.-H. Lin, and Q. Chen, "Characterizing exhaled airflow from breathing and talking," *Indoor Air* **20**(1), 31 (2010).
- ⁴⁵C. Pörschmann, T. Lübeck, and J. M. Arend, "Impact of face masks on voice radiation," *J. Acoust. Soc. Am.* **148**(6), 3663–3670 (2020).
- ⁴⁶G. Boiger, "Development and verification of a novel Lagrangian, (non-)spherical dirt particle and deposition model to simulate fluid filtration processes using OpenFOAM" (2009).
- ⁴⁷S. B. Martin, Jr., R. B. Lawrence, and K. R. Mead, "Evaluation of environmental controls at a faith-based homeless shelter associated with a tuberculosis outbreak – Texas," Report No. 2013-0110-3218, U.S. Department of Health and Human Services, 2014.
- ⁴⁸C. C. Coffey, J. B. Hudnall, and S. B. Martin, "Improving the environmental controls at a homeless shelter to assist in reducing the probability of airborne transmission of mycobacterium tuberculosis: A case study," *Indoor Built Environ.* **18**(2), 168 (2009).